Global Change Biology (2006) **12,** 777–792, doi: 10.1111/j.1365-2486.2006.01111.x

# Dynamical effects of the statistical structure of annual rainfall on dryland vegetation

CHRISTOPHER A. WILLIAMS*† [1] and JOHN D. ALBERTSON*†
*Civil and Environmental Engineering, Duke University, Durham, NC, 27708-0287, USA,
†Nicholas School of the Environment and Earth Sciences, Duke University, Durham, NC, 27708-028, USA

**Abstract**

**In this study, we extend a model of daily dryland dynamics by parameterizing a modified version of a minimalistic annual model to examine how the statistical structure of annual rainfall and grazing intensity interact to influence dryland vegetation. With a Monte Carlo approach, an ensemble outcome provides a statistical description of likely dryland vegetation dynamics responding to variations in rainfall structure and grazing intensity. Results suggest that increased rainfall variability decreases the average and increases the variability of grass cover leading to more frequent degradation of the grass resource. Vegetation of drier regions is found to be more sensitive to interannual variability in rainfall. Concentrating this variability into an organized periodic mode further decreases the mean and increases the variability of grass cover. Hence, a shift toward lower, more variable, or more inter-annually correlated annual rainfall will likely lead to a general decrease in the grass resource and increased dryland vulnerability to degradation.**

**Higher grazing intensity or lower annual rainfall both lead to more frequent and longer duration degradation of the grass condition. We note an interesting interaction in the response of grass biomass to grazing intensity and rainfall variability, where increased rainfall variability leads to longer duration degradation for low grazing, but shorter periods of degradation for high grazing. Once grass reaches a degraded condition, we find that woody vegetation strongly suppresses recovery even if successive rainfall is high. Overall, these findings suggest that the projected increase in interannual rainfall variability will likely decrease grass cover and potentially lead to more frequent, longer lasting degradation of dryland vegetation, particularly if enhanced rainfall variability is concentrated in long period (e.g. decadal) modes.**

*Key words:* desertification, drought, ensemble analysis, grazing, rainfall variability, vegetation dynamics, woody encroachment

*Received 14 July 2005; and accepted 29 September 2005*

## Introduction

Dryland ecosystems are generally thought to be highly susceptible to degradation by drought, overgrazing, or changes in fire regime, resulting in possible desertification, deforestation, or woody encroachment (Archer, 1989; Grover & Musick, 1990; Schlesinger, 1990; Manzano *et al.*, 2000; Gonzalez, 2001; Roques *et al.*, 2001; Scheffer & Carpenter, 2003). Degradation of drylands threatens fuelwood, forage, freshwater and other services important for global food supply, particularly for impoverished pastoral and agricultural populations worldwide (Scholes & Archer, 1997). Their vast terrestrial coverage (Atjay *et al.*, 1979) makes their potential change also significant, though uncertain, for global water and carbon cycles (Fisher *et al.*, 1994; Cao *et al.*, 2001; Jackson *et al.*, 2002). Therefore, it is vital that we understand the variables that control dynamics of dryland vegetation, especially in the context of a likely change in climate.

It is widely known that dryland vegetation is sensitive to daily to decadal rainfall variability (e.g. Noy-Meir, 1973; Knapp *et al.*, 2002; Chesson *et al.*, 2004),

Correspondence: Christopher A. Williams, tel. 970-491-1964, fax 970-491-1965, e-mail: caw@nrel.colostate.edu
[1]Present address: Natural Resource Ecology Laboratory, Colorado State University, Fort Collins, CO 80523-1499, USA.

though it remains unclear how this sensitivity interacts with land use factors such as grazing or fire management (Jeltsch *et al.*, 2000). Threshold or state-and-transition models of dryland vegetation suggest that both local disturbances (fire, grazing) and extreme climate events (droughts) regulate vegetation transitions between equilibrium states (e.g. Noy-Meir, 1975; Walker *et al.*, 1981; Westoby *et al.*, 1989; West, 1993). These conceptual models emphasize how internal positive feedbacks may lead to multiple preferential states, providing possible explanations of observed rapid, and potentially irreversible, dryland vegetation change (Noy-Meir, 1975; Walker *et al.*, 1981; van de Koppel *et al.*, 1997). However, such models are unable to quantify the likelihood of actual transitions, arguably because of inadequate representation of temporal variation in environmental conditions, particularly rainfall.

Rainfall is highly variable in dryland systems, with sporadic daily pulses, marked seasonality, and interannual to multi-decadal fluctuations (Noy-Meir, 1973; Chesson *et al.*, 2004). Dryland vegetation production as well as cover are strongly correlated with seasonal and longer variation in precipitation (Lauenroth & Sala, 1992; Milchunas *et al.*, 1994; Grist *et al.*, 1997). In fact, Ellis & Swift (1988) suggest that high interannual variability in rainfall may maintain dryland ecosystems in a perpetual non-equilibrium state. Thus, models of dryland vegetation dynamics need to capture effects of temporal variability in rainfall including interannual to decadal timescale oscillations. Furthermore, rainfall variability is predicted to increase globally at daily to decadal time scales (Karl *et al.*, 1995; Easterling *et al.*, 2000; IPCC, 2001). We explore in this paper the likely effects of such changes in rainfall variability.

Observational studies evaluating dryland vegetation responses to interannual rainfall variability are few, since dryland vegetation change can be slow (decadal time scale), rainfall is highly variable, and extreme events can be important (Scholes, 1990). Additionally, conclusions from such observational studies are often contradictory, perhaps because of confounding effects from other variables such as land use and disturbance. For example, Fuhlendorf *et al*. (2001) found plant basal area and total plant density to be correlated with annual precipitation in a 44-year record, suggesting that long-period climate trends exert significant control on year-to-year vegetation change. In contrast, Anderson & Inouye (2001) reported that neither shrub nor grass cover was significantly correlated with annual rainfall over a 45-year record despite vegetation and climate similar to that in Fuhlendorf *et al*. (2001). Even if observational studies provided a consistent picture, they are still restricted to describing an often-narrow range of environmental conditions observed in a specific sequence. Hence, in this study, we turn to a modeling approach for more extensive sensitivity analysis of long-term vegetation dynamics.

To date, only a few models representing dryland vegetation dynamics have been applied to examine likely effects of interannual variability in rainfall. Pickup (1996) studied the sensitivity of rangeland vegetation to variability in annual rainfall for a 50-year record with a simplistic model of grazing and rain-driven grass production. Results suggest that interannual variability in rainfall is the dominant control on grass production, though high grazing intensity increases the likelihood of grass degradation by drought (Pickup, 1996). With a rule-based automata model of an Australian dryland system Wiegand & Milton (1996) found that vegetation states were not only influenced by the amount but also the temporal pattern of monthly rainfall for a series of century-scale simulations. While revealing, these studies examine a narrow range of the possible grazing and rainfall conditions and may lack some of the important features that influence dryland vegetation states. For example, the statistical structure of rainfall's interannual correlation has been neglected, calling for a more comprehensive investigation.

Here, we study how mean annual rainfall, interannual variability of rainfall, and the organization of this variability (i.e. interannual correlation) interact with grazing to influence grass and wood covers and the probability of savanna conversion to a state of desertification or woody encroachment. We accomplish this through addressing several open research questions:

- How sensitive are grass dynamics to interactions between grazing intensity, mean annual rainfall, and interannual rainfall variability?
- To what degree do long period modes of interannual rainfall variability contribute to grass dynamics?
- To what degree does wood suppression of grass limit the potential for grass recovery following degradation?

We address these questions with a numerical model based on an existing framework describing wood, grass, grazing, and fire interactions in water-limited ecosystems (Anderies *et al.*, 2002). We use the model to study dynamical effects of the statistical structure of annual rainfall on dryland vegetation. In previous work, we examined how vegetation–atmosphere exchanges of water and carbon are controlled by soil moisture (Williams & Albertson, 2004) and may be influenced by vegetation structural dynamics typical of southern African savannas (Williams & Albertson, 2005). We use these prior results to parameterize the present model for study of the southern African region,

but note that this does not prohibit broader application of our findings to water-limited ecosystems, in general.

## Methods

### *Model*

We begin by adopting and modifying the annual time-step, dynamical systems model of grass (herbaceous) and wood (shrub and tree) vegetation types in rangelands outlined by Anderies *et al*. (2002) to include the following additional components typical of dryland dynamics. We consider effects of interannual variability in rainfall on grass and wood growth rates and carrying capacities as described in Appendix A. We also consider grass competitive effects on wood production and the reverse, unlike the previous framework (Anderies *et al*., 2002), which considered only wood on grass competitive effects. We include fire occurrence as a stochastic rather than deterministic process, and allow fire intensity to depend on both grass and wood biomass, as described in Appendix B, rather than just grass biomass as in the original formulation (Anderies *et al*., 2002). With these modifications the model for grass ($G$), grass root ($R$), and wood ($W$) biomass states is

$$\begin{aligned}\frac{dG}{dt} &= \min\left(\frac{R}{R_*}, 1\right)(\eta + r_g G)\left(1 - \frac{G}{k_g} - \alpha_w \frac{W}{k_w}\right) - L_g G - FB_g G,\\ \frac{dR}{dt} &= r_r G - L_r R,\\ \frac{dW}{dt} &= r_w W\left(1 - \frac{W}{k_w} - \alpha_g \frac{G}{k_g}\right) - FB_w W.\end{aligned} \tag{1}$$

Table 1 presents symbols and units.

The model describes competition and density-dependent logistic growth of grass biomass ($G$, kg grass dry matter (DM) $m^{-2}$ ground), and wood biomass ($W$, kg wood DM $m^{-2}$ ground). Interannual rainfall fluctuations influence grass and wood carrying capacities ($k_g$, $k_w$,

**Table 1** Variables, parameters and functions in the annual model

| Symbol | Description (units) | Value |
|---|---|---|
| $< >$ | Time average operator | – |
| $\sigma$ | Standard deviation operator | – |
| CV( ) | Coefficient of variation operator | – |
| $G$, $R$, $W$ | Grass shoot, grass root, and wood biomass (kg DM $m^{-2}$) | 0–6 |
| $R_*$ | Root biomass at full resource extraction potential (kg DM $m^{-2}$) | $0.1G_{max}$ |
| $G_{cr}$, $R_{cr}$ | Grass and root biomass threshold of recovery (kg DM $m^{-2}$) | 0.3 |
| $\eta$ | Resprout rate for grass shoots ($year^{-1}$) | 0.2 |
| $r_g$, $r_r$, $r_w$ | Growth rate ($year^{-1}$) | 0.2–1.5 |
| $r_{gmax}$, $r_{wmax}$ | Maximum growth rate ($year^{-1}$) | 1.2, 0.4 |
| $k_g$, $k_w$ | Carrying capacity for grass and wood (kg DM $m^{-2}$) | 2–6 |
| $\alpha_{wg}$, $\alpha_{gw}$ | Competition coefficients (dimensionless) | 0.5 |
| $L_g$ | Grazing rate ($year^{-1}$) | 0–1 |
| $F$ | Annual fire occurrence (dimensionless) | 1, 0 |
| $B_g$, $B_w$ | Burn completeness (fraction of DM $yr^{-1}$) | 0.1–1 |
| $L_r$ | Root decay rate ($year^{-1}$) | 0.2 |
| $a_g$, $a_w$ | Slope of intrinsic growth rate with annual rainfall ($year^{-1}$) | 0.0029, 0.0008 |
| $b_g$, $b_w$ | Intercept of intrinsic growth rate with annual rainfall ($year^{-1}$) | −0.17, 0.032 |
| $c_g$, $c_w$ | Slope of carrying capacity with annual rainfall (kg DM $m^{-2}$) | 0.0028, 0.0048 |
| $d_g$, $d_w$ | Intercept of carrying capacity with annual rainfall (kg DM $m^{-2}$) | 0.59 |
| $P$ | Annual rainfall (mm) | 0–2000 |
| $T_f$ | Mean return time of fire (year) | 1–30 |
| $C_g$, $C_w$ | Combustion completeness factor (fraction of DM) | 1, 0.5 |
| $f_v$ | Vegetation fractional cover ($m^2$ vegetated area $m^{-2}$ ground area) | 0–1 |
| $G_{max}$, $W_{max}$ | Grass shoot or wood biomass at full vegetation fractional cover (kg DM $m^{-2}$) | 2, 6 |
| $h_g$, $h_w$ | Point at which biomass consumption by fire is half its maximum (dimensionless) | 0.2, 0.5 |
| $e_g$, $e_w$ | Sharpness of the threshold for biomass consumption by fire (dimensionless) | 1, 3 |
| $\gamma$ | Fraction of annual rainfall variance that is uncorrelated | 0–1 |
| $U$ | Uncorrelated, lognormally distributed random variable | 0–1500 |
| $A_p$ | Amplitude of periodic oscillations in annual rainfall (mm) | 0–300 |
| $T_p$ | Period of periodic oscillations in annual rainfall (year) | 0–33 |

Subscripts g, r, w, wg, gw, and $x$ refer to grass, root, wood, effect of wood on grass, effect of grass on wood, and either g or w as appropriate.

kg DM $m^{-2}$) and grass, grass root, and wood growth rates ($r_g$, $r_r$, $r_w$, $yr^{-1}$). Competition coefficients ($\alpha_g$, $\alpha_w$) describe grass and wood competition for soil moisture. Stochastic fire disturbances, $F$ (dimensionless), remove grass or wood dry matter according to biomass combustion factors ($B_g$, $B_w$, $yr^{-1}$). Though grazing pressure may fluctuate in time with herbivore populations, we restrict this first analysis to maintaining a static grazing rate ($L_g$, $yr^{-1}$) for each simulation, as in the original model (Anderies *et al.*, 2002). Root biomass ($R$, kg grass root DM $m^{-2}$) governs the potential for $G$ recovery from a low state, and $R$ decays at a fixed rate ($L_r$, $yr^{-1}$). Consecutive years of low $G$ can lead to the net decay of $R$, limiting the potential for regrowth of $G$ if $R < R_*$, a parameter describing the potential for root resource extraction, and potentially leading to $G$ extinction ($G = 0$, $R = 0$). Since recolonization and regrowth following disturbance can be rapid (e.g. Trollope *et al.*, 1996), and grass extinction is rare, except possibly on a local scale (O'Connor, 1991), we introduce an additional recolonization mechanism, such that after two consecutive years of $G < G_{cr}$ and $R < R_{cr}$, $G$ and $R$ are reset to $G_{cr}$, $R_{cr}$. The value $G_{cr}$ is also used as a threshold describing degradation of the grass condition in the sections *Interaction of grazing and rainfall effects* and *Recovery from degradation*.

Despite the model's minimalistic nature, this representation provides a useful tool for exploring the sensitivity and potential responses of dryland vegetation to perturbations in land use management or rainfall regime. We emphasize that our goal is not to represent a specific dryland ecosystem, or to predict a future trajectory of a particular water-limited system, but rather to study how the temporal structure of annual rainfall variation may interact with grazing to influence grass and wood states.

### *Numerical experiments*

Two sets of numerical simulations were conducted, each addressing a specific objective. The first objective is to assess how grass dynamics respond to differing degrees of grazing intensity ($L_g$), mean annual rainfall ($<P>$), and interannual variability of rainfall represented by the coefficient of variation of rainfall (CV($P$)), where $<>$ is the time-average operator computed over simulation years unless specified otherwise, and the coefficient of variation is computed as the interannual standard deviation, $\sigma_P$, divided by the mean, as $CV(P) = \sigma_P / <P>$. To control the statistical structure of annual rainfall, we generate synthetic $P$ time series, represented as

$$P_t = \langle P \rangle + U_t + A_p \sin\left(\frac{2\pi t}{T_p}\right), \qquad (2)$$

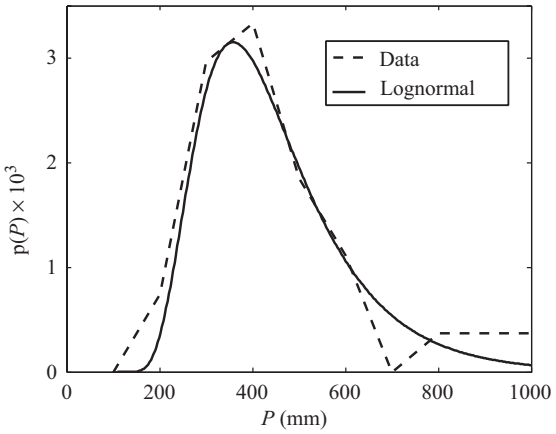


**Fig. 1** Lognormal probability ($P$) distribution (—) used to approximate the observed distribution (- - -) of annual rainfall ($P$) for the Ghanzi, Botswana rainfall dataset.

where $t$ is time, $U_t$ is an uncorrelated, lognormally distributed random variable with variance $\gamma\sigma_P^2$, where $\gamma$ is a parameter (0 to 1) controlling the partitioning of total variance ($\sigma_P^2$) between the uncorrelated (white) and correlated (here, sinusoidal) components, $A_p (= \sqrt{2(1-\gamma)\sigma_P^2})$ is the sinusoidal amplitude (mm), and $T_p$ is the period (yr). The lognormal distribution is chosen as a good approximation to an observed frequency distribution of total annual rainfall based on analysis of a daily rainfall record from central Botswana (Eaton, unpublished). The record extends from 1972 to 2002 for a site near Ghanzi, Botswana indicating mean annual rainfall of $\sim 450$ mm, and a coefficient of variation of $\sim 0.4$ (Fig. 1). We use Eqn (2) to construct synthetic annual rainfall time series with desired mean, variance, and correlation statistics for both numerical experiments.

In the first simulation set, $P$ series are absent of sinusoidal forcing ($\gamma = 1$) such that $P$ has a random (white noise) structure. With these unstructured annual rainfall series, we study a full factorial combination of $L_g$, $<P>$, and CV($P$) with stochastic fire events, as detailed in Table 2. Ranges of $<P>$ and CV($P$) are selected to broadly sample conditions representative of water-limited ecosystems. Le Houérou *et al.* (1988) showed CV($P$) to range from $\sim 0.1$ to $\sim 0.6$ for 77 sites in arid to semi-arid rangelands worldwide. Grazing intensity ranges from 0 to $\sim 0.6$ $yr^{-1}$ with the highest rates typical of communal grazing and $\sim 0.3$ $yr^{-1}$ common to commercial operations (Pickup, 1996; Fynn & O'Connor, 2000; Anderies *et al.*, 2002). Results from the first simulation set are presented in sections *Sensitivity to $<P>$ and CV(P)* and *Interactions of grazing and rainfall effects*. A sub-sample of the first simulation set is also used to investigate the degree to which drought

**Table 2** Parameter and statistic values used in simulation sets 1 and 2 for grazing intensity, mean annual rainfall, coefficient of variation of $P$, the fraction of $P$ variance in the periodic mode, the time period ($T_p$) of the periodic mode, initial grass and wood states, potential fire states, the number ($N_{sim}$) of simulations in each ensemble, and the number of simulated years ($N_{yr}$) for each individual trajectory

| Parameter/statistic | Set 1 | Set 2 |
|---|---|---|
| $L_g$ (year$^{-1}$) | 0, 0.1, 0.2, 0.3, 0.4, 0.5, 0.6, 0.7, 0.8 | 0.1, 0.2, 0.3, 0.4 |
| $<P>$ (mm) | 350, 450, 550, 650 | 350, 450, 550 |
| CV($P$) | 0, 0.1, 0.2, 0.3, 0.4, 0.5, 0.6, 0.7, 0.8 | 0.1, 0.2, 0.3, 0.4 |
| Fraction of $\sigma_P^2$ in mode | 0 | 0, 0.2, 0.4, 0.6, 0.8, 1 |
| $T_p$ (year) | 0 | 5, 33 |
| Initial $G$, $W$ (kg DM m$^{-2}$) | 1, 1 | 1, 1 |
| $F$ | Yes | No |
| $N_{sim}$ | 100 | 100 |
| $N_{yr}$ | 100 | 100 |

and competition for soil moisture influence grass recovery from a degraded state in section *Recovery from degradation*.

The second objective is to assess the sensitivity of grass dynamics to low-frequency modes of rainfall (i.e. the degree of memory ($1-\gamma$) in the year-to-year rainfall series). For this purpose, the second simulation set evaluates responses to a factorial combination of $L_g$, $<P>$, CV($P$), and the desired fraction ($1-\gamma$) of annual rainfall variance concentrated in the organized (correlated) mode, also detailed in Table 2. Fire is suppressed ($F = 0$) in this set to permit a more clear characterization of how periodic rainfall alone may force dryland vegetation dynamics. Results from simulation set 2 are presented in the section *Sensitivity to long period rainfall modes*.

Owing to the random term in Eqn (2), we adopt a Monte Carlo approach using ensembles of simulations (all with the same initial conditions) to characterize ranges of possible response and relative likelihood. As such, each $L_g$–$<P>$–CV($P$) combination in the first simulation set, and each $L_g$–$<P>$–CV($P$)–$\gamma$ combination in set two are simulated with 100 separate runs (ensembles of 100) with each run lasting 100 years. The initial conditions are selected to prevent initial competitive dominance of wood or grass as well as to prevent initial grass degradation, and is representative of $\sim 60\%$ grass cover ($G \sim 1.2$ kg DM m$^{-2}$) and $\sim 20\%$ wood cover ($W \sim 1.2$ kg DM m$^{-2}$), in accordance with Williams & Albertson (2005).

## Results and discussion

### *Deterministic dynamics*

Before proceeding with our numerical analysis, it is instructive to evaluate the deterministic dynamics of this system of equations to highlight potential sensitivity of vegetation to grazing and annual rainfall. We study equilibrium solutions for high, low, and intermediate fixed annual rainfall with fire suppression ($F = 0$), thus removing stochasticity from the system, and for a low grazing intensity ($L_g = 0.1$ yr$^{-1}$). We apply the traditional stability analysis of linearizing around fixed points with a Taylor series expansion to evaluate fixed point stability with the characteristic equation and using an eigenvalue–eigenvector solution to obtain the stable and unstable manifolds (Roughgarden, 1979; Edelstein-Keshet, 1988). Graphically, we see that intersections of the grass biomass ($G$) and root reserves ($R$) isoclines produce two stable and one unstable fixed points for conditions of intermediate ($P = 415$ mm) and high ($P = 1000$ mm) fixed annual rainfall (Fig. 2a), though the high biomass stable fixed point for high rainfall is not shown as it is located at $G = 2.4$ kg DM m$^{-2}$, $R = 2.4$ kg DM m$^{-2}$. If rainfall is adequate, a stable manifold, or separatrix, divides the state space into two basins of attraction, one supporting abundant grass, and one tending toward grass extinction (Fig. 2a). Similar to the effect of decreased grazing intensity as presented by Anderies *et al*. (2002), we find that increasing fixed annual rainfall from 415 to 1000 mm shifts the stable manifold to the left (toward lower $G$), shrinking the basin that leads to grass extinction. Decreasing fixed annual rainfall from 415 to 200 mm shifts the $G$-isocline up and to the left (toward lower $G$) causing the high grass biomass basin to vanish.

Figure 2b presents a bifurcation diagram of grass biomass as a function of rainfall. Two fixed points exist for high annual rainfall, however the high biomass fixed point vanishes abruptly for annual rainfall below a critical value, as illustrated in Fig. 2b for $L_g = 0.3$ yr$^{-1}$ at $P \sim 420$ mm. These results are consistent with those

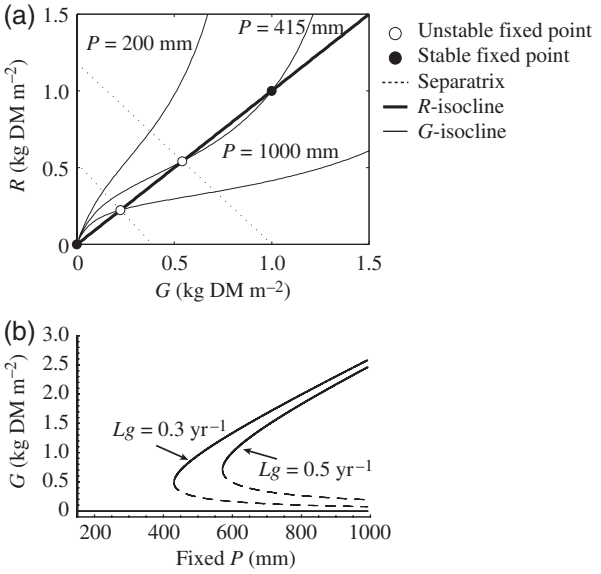


**Fig. 2** (a) Fixed point, isocline, and separatrix solutions obtained from linear stability analysis of Eqn (1) plotted in the root reserve vs. grass biomass (*R*–*G*) state space for three conditions of annual rainfall (*P*) with low grazing intensity ($L_g = 0.2\,\mathrm{yr}^{-1}$), and (b) bifurcation diagram of the *G* fixed points as a function of *P* for two levels of grazing intensity, where the solid and dashed lines indicate stable and unstable fixed points, respectively.

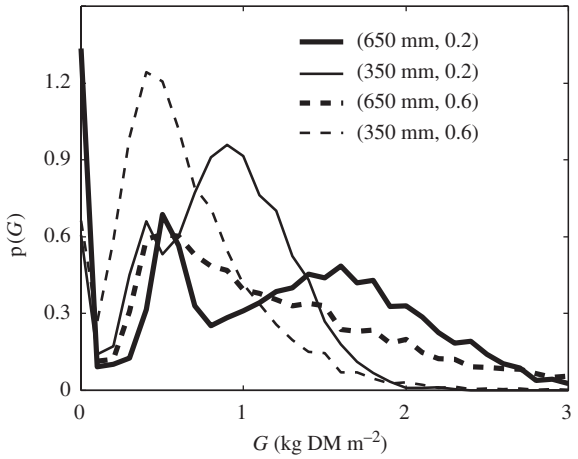


**Fig. 3** Probability (*P*) distributions of grass biomass (*G*) from 100-year ensemble simulations with different combinations of mean and coefficient of variation of annual rainfall, presented in the legend as {<*P*>, CV(*P*)}, and for a grazing intensity of $0.2\,\mathrm{yr}^{-1}$.

reported by van de Koppel & Rietkerk (2004) who modified the Walker *et al*. (1981) formulation of savanna dynamics, documenting a similar bifurcation of grass biomass as a function of rainfall rate. In addition, we find that increased grazing intensity shifts to the right the critical rainfall at which the high grass biomass fixed point appears and expands the basin of attraction for the $G = 0$ fixed point, qualitatively similar to effects of grazing on grass stability described in Walker *et al*. (1981).

From this initial analysis we demonstrate how both high and low ($G = 0$) grass stable states may exist for a single fixed annual rainfall. Demarcating basins of attraction for each fixed point given static (fixed) rainfall conditions can be useful for conceptualizing the underlying system dynamics, including the potential for fast shifts, 'irreversibility', and extinction. However, the stable states are sensitive to rainfall through its effect on $r_x$ and $k_x$, indicating that a shift from a high to low rainfall regime may cause an abrupt collapse of grass, and hence the forage resource. Despite having documented sensitivity of equilibrium solutions to fixed annual rainfall, it remains unclear how the system will respond to interannual variability in rainfall. This motivates numerical simulation for studying the effects of variability in annual rainfall on grass biomass.

### *Sensitivity to* <P> *and CV(*P)

To examine the sensitivity of dryland vegetation to variation in the mean and variance of annual rainfall, we study results from the first simulation set, described in section *Numerical experiments*. Stochastic forcings of precipitation (uncorrelated) and fire spread the ensemble outcome of grass biomass, evidenced by broad probability distributions of grass biomass (Fig. 3) obtained from the 100 runs × 100 years for each parameter set. Wetter conditions (<*P*> = 650 compared to 350 mm) broaden the grass biomass distribution. More variable annual rainfall (CV(*P*) = 0.6 compared to 0.2) shifts the mode toward lower values (Fig. 3). Additionally, effects of mean and variance interact, as the grass biomass distribution appears to be less sensitive to the degree of annual rainfall variability for wetter as compared to drier conditions (Fig. 3). Fires cause the mode near zero grass biomass; however, grass recovers rapidly if root reserves (*R*) are sufficient. Modes near $G \sim 0.3$ result, in part, from a model artifact in which we reset *G* to $G_{cr}$ to simulate recolonization (Fig. 3).

Exploring further the sensitivity of grass biomass to variability in annual rainfall, Fig. 4 presents the average grass biomass computed over simulation years, <*G*>, and averaged over the ensemble of runs for each parameter set, denoted with an overbar as $\overline{<G>}$. The ensemble-averaged coefficient of variation for grass, $\overline{CV(G)}$, is also shown, each for a range of <*P*> and CV(*P*) conditions and for low and intermediate grazing intensities. Note that we omit results for <*P*> = 350 mm with $L_g = 0.3\ \mathrm{yr}^{-1}$ since *G* and *R* remain at or below the critical *G* and *R* states, and hence, the

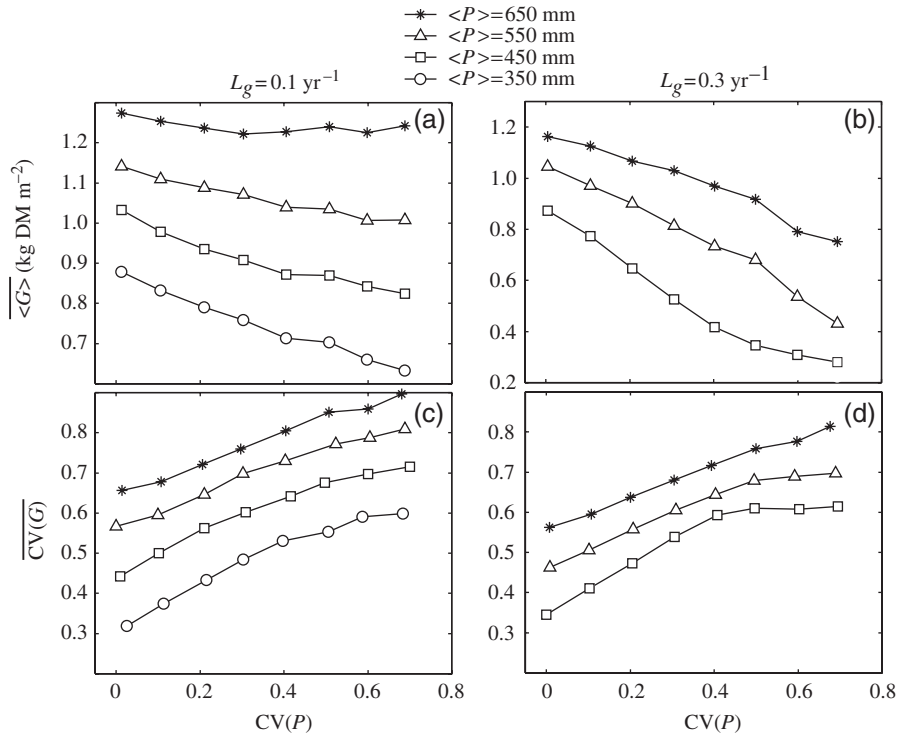


**Fig. 4** Mean (a, b) and coefficient of variation (c, d) of grass biomass ($G$) evaluated over simulation years and averaged across ensemble simulations for low (a, c) and intermediate (b, d) grazing intensity ($L_g$) vs. the coefficient of variation of annual rainfall ($P$), for four conditions of mean annual rainfall ($<P>$).

mean and variation of $G$ reflect an artifact of modeled recolonization.

In general, a wetter rainfall regime increases grass biomass while a more variable rainfall regime decreases grass biomass (Fig. 4a, b). Both higher and more variable rainfall increase the variability of grass biomass (Fig. 4c, d). Mean grass biomass is more sensitive to rainfall variability for lower mean annual rainfall, particularly for low grazing intensity (Fig. 4a). These results support the view (Wiens, 1984; Ellis & Swift, 1988) that vegetation of drier regions (lower $<P>$) is more sensitive to interannual variability in rainfall and more vulnerable to transition to a degraded state by interannual rainfall fluctuations. Furthermore, our findings suggest that a shift toward more variable rainfall conditions could lead to a general decrease in grass cover, and hence, threatens grazing resources.

Modeled grass biomass fluctuates at approximately 40% of the rate of fluctuations in annual rainfall, as apparent from the slopes in Fig. 4c, d. Grass responses to rainfall perturbations are limited by both the initial grass state and characteristic growth rate, consistent with Lauenroth & Sala (1992) and Paruelo *et al*. (1999). Grass biomass fluctuations are also excited by fire, carrying-capacity-related grass biomass regulation, and competitive interactions as evidenced by normalized grass biomass fluctuations (CV($G$)) that exceed normalized rainfall fluctuations (CV($P$)) (Fig. 4c, d), consistent with worldwide observations (Le Houérou *et al*., 1988) of the variability of annual dryland production.

Increased grazing intensity reduces both the mean and variability of grass biomass (Fig. 4), particularly noticeable when noting the change in $y$-axis range of panels a and b. Increased grazing intensity also increases grass sensitivity to rainfall variability even for high rainfall ($<P> = 650$ mm) (Fig. 4a, b). The combination of overgrazing and low rainfall ($<P> = 350$ mm and $L_g = 0.3$ yr$^{-1}$, not shown) provides an exception to this trend, as grass biomass is reduced to a perpetually low state.

### *Interaction of grazing and rainfall effects*

To more closely investigate the interaction of grazing and rainfall effects, next we explore how grazing, and the mean and variance of annual rainfall jointly influence grass biomass. Rather than studying the mean grass state, studies of grazing and rangeland conditions often focus on the likelihood of degrading the grass resource, since punctuated degradation events can be long lasting with a substantial effect on long-term

productivity. Therefore, we study the frequency of grass being below a critical threshold, $G_{cr}$, representing the frequency of desertification or woody encroachment, hereafter called degradation frequency, $\xi$, computed as

$$\xi = \frac{\sum_{j=1}^{N_{sim}} \sum_{i=1}^{N_{yr}} x_{ij}}{N_{sim} N_{yr}}, \quad (3)$$

where

$$X_{ij} = \left\{ \begin{array}{ll} 1 & \text{for } G_{ij} \leq G_{cr} \\ 0 & \text{otherwise} \end{array} \right\}, \quad (4)$$

and $G_{ij}$ is $G$ of the $i$th year in the $j$th simulation, $N_{sim}$ is the number of simulations in an ensemble ( = 100), $N_{yr}$ is the number of years of a simulation ( = 100) for each $L_g$–<$P$>–CV($P$) combination. In addition, we quantify the mean duration of degradation ($T_\xi$, yr) as

$$T_\xi = \frac{\sum_{j=1}^{N_{sim}} \sum_{z=1}^{N_j} k_* - k_{z,j}}{\sum_{j=1}^{N_{sim}} N_j}, \quad (5)$$

following each degradation event, $z$, defined as ($G_{i,j} \leq G_{cr} \mid G_{i-1,j} > G_{cr}$) and where $k_{zj}$ is the year of the $z$th degradation event, in the $j$th simulation, $N_j$ is the number of such events in the $j$th simulation, and $k_*$ is the year of the first $G > G_{cr}$ after $k_{zj}$. These measures provide an indication of grass vulnerability to degradation by the joint effects of overgrazing, fire, woody encroachment, and rainfall fluctuations.

The frequency of grass degradation increases with both increased grazing intensity and increased variability in rainfall, though grass is more resistant to degradation in a high rainfall regime (Fig. 5a, b). Hence, higher grazing intensity can be sustained on sites with less variable or higher mean annual rainfall, consistent with prior findings that document a narrower range of rainfall conditions (e.g. Pickup, 1996; Wiegand & Milton, 1996). The frequency of degradation is less sensitive to rainfall variability in low rainfall or high grazing conditions (Fig. 5a, b) indicating that either a low initial grass biomass state or overgrazing inhibit grass recovery during wet years.

Not surprisingly, degradation tends to be of longer duration for high grazing or low mean annual rainfall (Fig. 5c, d). But what is interesting is that increased variability of annual rainfall leads to longer duration degradation for low grazing but shorter periods of degradation for high grazing (Fig. 5c, d). This can be explained from the basic observation that the annual rainfall needed to enable grass recovery from a degraded state (denoted $P_{cr}$) is larger in the presence of high compared to low grazing intensity. Thus, if grazing

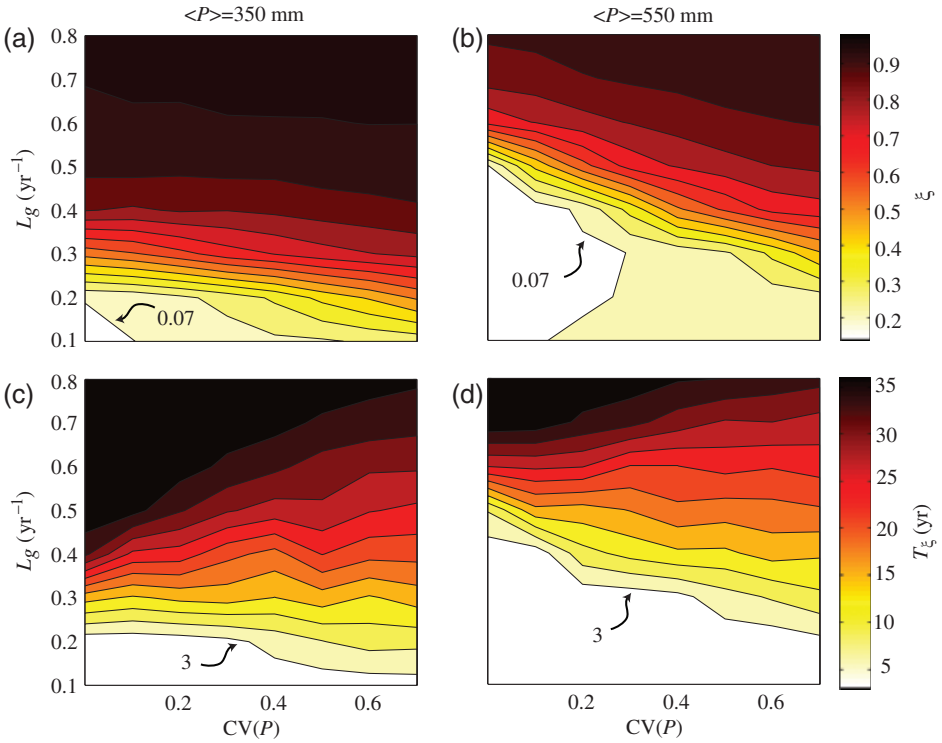


**Fig. 5** Frequency of degradation, $\xi$ (a, b) and mean duration of degradation, $T_\xi$ (c, d) contoured over grazing intensity ($L_g$) and the coefficient of variation of $P$ for low (a, c) and high (b, d) mean annual rainfall. Contour intervals are 0.07 and 3 for panels a, b and c, d, respectively.

intensity is low, nearly the entire distribution of $P$ may be above the $P_{cr}$ for grass recovery from degradation, such that increasing the variability of $P$ would cause more of the $P$ distribution to fall below this critical level and leading to longer duration degradation on average. In contrast, if grazing intensity is high, nearly all of the $P$ distribution may lie below $P_{cr}$, such that increased CV($P$) would cause more of the $P$ distribution to lie above $P_{cr}$, thus decreasing the average duration of grass degradation.

Overall, these results suggest that increased variability of rainfall is likely to result in less grass biomass and more frequent and longer lasting periods of woody encroachment and desertification. While consistent with those of Pickup (1996) and Wiegand & Milton (1996), our results address a broader range of rainfall and grazing combinations providing a wider view of possible dryland responses. In this section we have studied how changing the random variance of annual rainfall may influence dryland vegetation states. However, in reality, observed rainfall often contains long period modes which have been hypothesized to be important in dryland vegetation dynamics (Noy-Meir, 1973; Ellis & Swift, 1988; Fuhlendorf *et al.*, 2001). We now explore how long period (correlated) modes of annual rainfall may influence grass biomass dynamics in drylands.

### *Sensitivity to long period rainfall modes*

To examine the influence of long period (correlated) modes of annual rainfall on dryland vegetation, we preformed the second set of simulations described in the section *Numerical experiments*, wherein we vary the variability of annual rainfall, as well as the fraction of that variation that is concentrated in a single, long period mode. First studying results in the absence of white noise fluctuations ($\gamma = 0$), Fig. 6 presents state–space representations of grass biomass and annual rainfall trajectories for simulations with varied CV($P$), which modulates the amplitudes ($A_p$) on a single, sinusoidal mode of $P$ with either a short ($T_p = 5$ years) or long ($T_p = 33$ years) period. Increasing the CV($P$) generally decreases the major axis (meaning the slope) of the $G$–$P$ relationship (Fig. 6) and decreases the mean and minimum $G$, as summarized in Fig. 7. This further supports the notion that $G$ is, on average, reduced by rainfall fluctuations, as found with white noise variability presented in the section Sensitivity to $<P>$ and CV($P$) (Figs 4 and 5). Additionally, grass biomass lags behind annual rainfall and is hysteretic in its response to annual rainfall, with a larger lag in growth compared to decay, particularly noticeable for the long period ($T_p = 33$ years) oscillation (Fig. 6). Greater lag in growth than decay can be partially attributed to characteristics of the logistic growth model used as the basis for Eqn (1). Initially slow growth for low grass biomass, as well as a unit growth rate ($r_g$) less than one for low annual rainfall (Appendix A) both contribute to lag during the growth phase. Wood competitive effects on grass may also contribute to slow grass recovery from a low grass biomass state, as examined in the section *Recovery from degradation*. Furthermore, the lag is less pronounced for the decay phase since decay rate scales with $G^2$ while the rate of growth scales with $G$. Correspondingly, a relatively long period of high rainfall may be required for grass recovery from even short-lived periods of low rainfall.

A longer period enables grass biomass to recover to a higher maximum following the low rainfall phase even with no change in annual rainfall variability (Fig. 7). Zeng *et al*. (2002) found a similar increase in vegetation

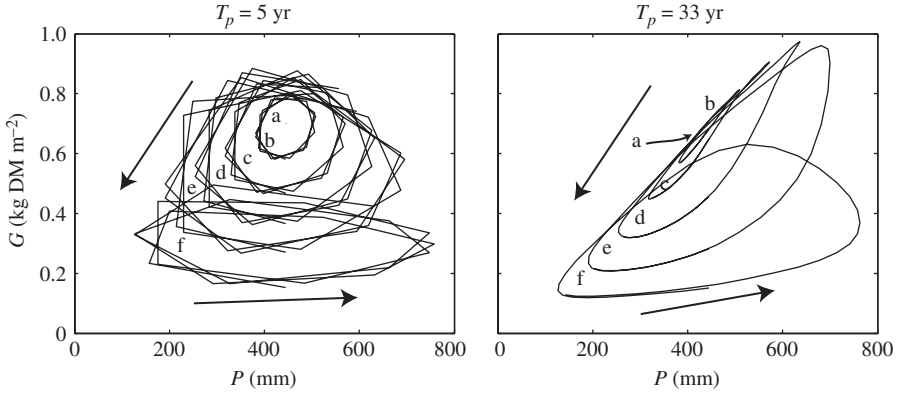


**Fig. 6** Grass biomass vs. annual rainfall ($G$–$P$) state–space portraits for the last 40 years of 100-year simulations with fire suppression ($F = 0$) and an intermediate grazing intensity ($L_g = 0.3\,\mathrm{yr}^{-1}$), and for mean annual rainfall of 450 mm. The letters a–f correspond to amplitudes of sinusoidal annual rainfall forcing of CV($P$) = 0, 0.1, 0.2, 0.3, 0.4, 0.5, respectively. Arrows indicate the direction of flow.

growth with increased period of annual rainfall forcing but with a more simplistic model of vegetation dynamics. Here, we also show that progressively lower minimum grass biomass with increased annual rainfall variability inhibits grass from fully responding to years with high annual rainfall (Fig. 6), consistent with the noted hysteresis. Hence, even if a period of low annual rainfall is followed by a long wet period, grass may be unable to fully recover to the state that would be realized in the absence of interannual rainfall variability.

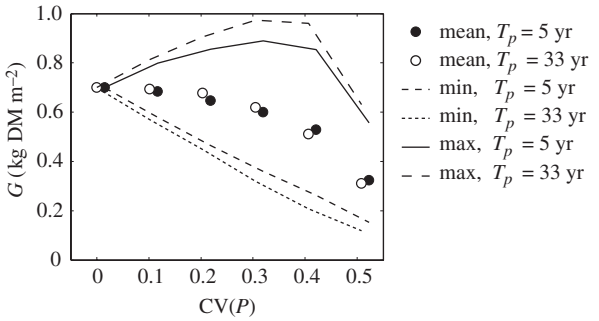


**Fig. 7** Mean, maximum, and minimum grass biomass ($G$) from the last 40 years of 100-year simulations vs. the coefficient of variation of annual rainfall (CV($P$)) for short (5-year) and long (33-year) periods of sinusoidal annual rainfall forcing, $T_P$, with fire suppression ($F = 0$), an intermediate grazing intensity ($L_g = 0.3\,yr^{-1}$), and for mean annual rainfall of 450 mm. For visual clarity, data from simulations containing a 5-year periodicity in $P$ were slightly shifted to the right.

Actual annual rainfall contains multiple modes of temporal variability rather than variability concentrated in a single periodic mode. In fact, it is hypothesized that high year-to-year variability may interrupt the potential influence of long period rainfall modes on vegetation states (Ellis & Galvin, 1994). Therefore, we study how the mean and coefficient of variation of grass biomass vary with the fraction of rainfall variability that is concentrated in a single mode as opposed to spread out as white noise in the spectrum. Increasing the fraction of annual rainfall variability concentrated in the periodic mode ($1-\gamma$) generally decreases the average grass biomass and increases its variability (Fig. 8). Also, our finding that an organized mode of larger period leads to even greater grass biomass variability but has little effect on the average grass state, as shown above (Fig. 7), is not altered by varying the correlated vs. uncorrelated distribution of annual rainfall variability (Fig. 8).

Taken together, large rainfall variance organized in a long-period mode causes the most pronounced reduc-

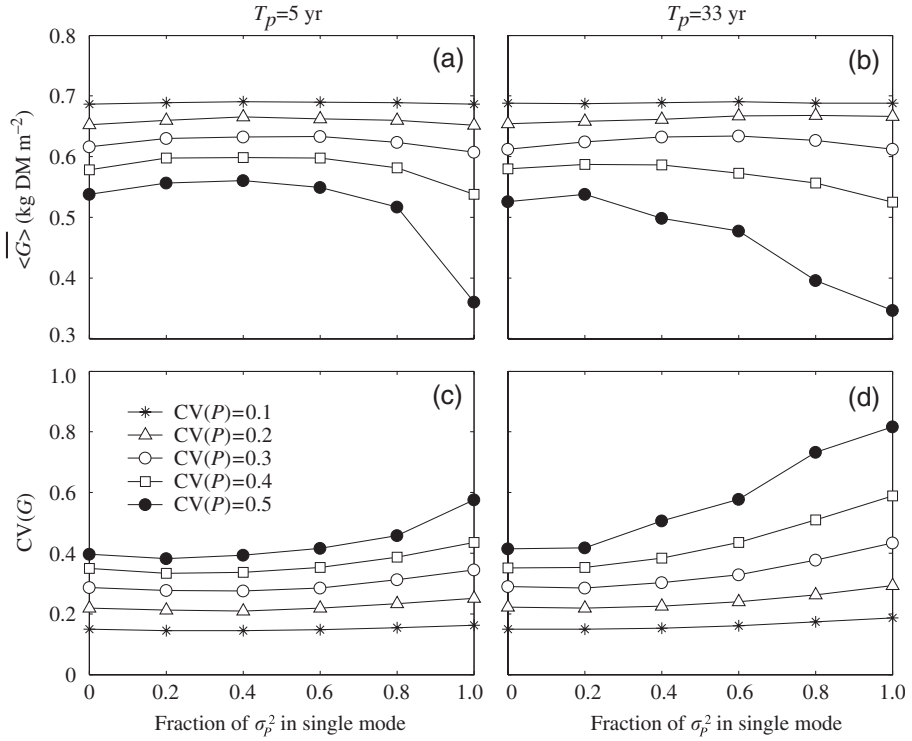


**Fig. 8** Mean (a, b) and coefficient of variation (c, d) of $G$ evaluated over simulation years and averaged across ensemble simulations vs. the fraction ($1-\gamma$) of annual rainfall variability concentrated in a single mode of a short (a, c) or long (b, d) period and for six conditions of annual rainfall variability (CV($P$)). Mean annual rainfall is 450 mm and grazing intensity is $0.3\,yr^{-1}$.

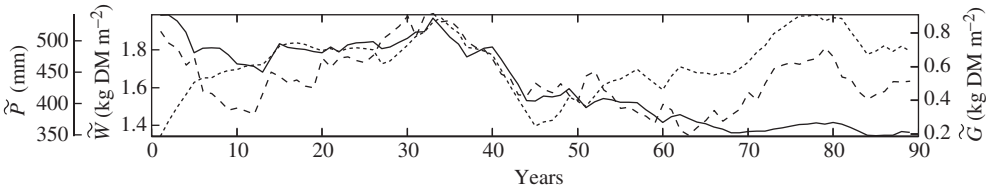


**Fig. 9** The 10-year moving averages of annual rainfall ($P$, - - -), wood biomass ($W$, . . .), and grass biomass ($G$, —) from a single case study.

tion in grass biomass and hence leads to the most likely degradation of the dryland vegetation state. These conditions result in the most coherent and prolonged dry periods threatening the loss of grass and potentially leading to desertification or woody encroachment. When combined with intense grazing, as examined in the previous section, the likelihood of grass degradation increases and recovery from overgrazing and dry periods may be slow, with a potentially long lag in recovery. These results are consistent with observed hysteresis in dryland systems (e.g. Friedel, 1991; Laycock, 1991; Ryerson & Parmenter, 2001) where decreased grass cover from drought or disturbance is more rapid than recovery with higher rainfall or with release from disturbance. In addition, modeled hysteresis and persistently low grass biomass with intense grazing and low rainfall lend support to the notion of 'irreversible', potentially catastrophic ecological change (Scheffer *et al.*, 2001, Wu & Marceau, 2002). Next, we analyze $G$, $W$, and $P$ trajectories to investigate how wood and drought combine to potentially limit the recovery of grass from a degraded state.

### *Recovery from degradation*

We have yet to consider the role of wood competitive effects on grass dynamics. While wood directly reduces grass growth Eqn (1), suppressing positive grass responses to rainfall and leading to more rapid grass decay, the presence of wood does not in itself preclude a high grass biomass state. We illustrate with a case study (single trajectory) from a 100-year simulation from simulation set 1 (white $P$ spectrum, $\gamma = 1$) with rainfall and grazing conditions representative of a commercial operation near Ghanzi, Botswana ($<P> =$ 450 mm, CV($P$) = 0.6, $L_g = 0.3$ yr$^{-1}$). We present 10-year moving averages of $P$, $W$, and $G$, to elucidate persistent trends (Fig. 9). A 10-year average is chosen because it is long enough to average out effects of individual fire events but short enough to preserve long-period dynamics in the time series.

For the first $\sim 50$ years of the case study, grass biomass ($\tilde{G}$) fluctuations largely follow those of annual rainfall ($\tilde{P}$). In contrast, wood biomass ($\tilde{W}$) generally increases for the first 30 years with relatively little influence from the annual rainfall fluctuations likely associated with a spin up from the initial condition, but from 30 to 50 years wood biomass declines with the persistent decrease in annual rainfall. Relatively low annual rainfall continued for years 50–70, leading to progressive gradual decay of grass biomass, while wood biomass gradually increases likely due to wood being released from grass competitive effects. Following this drought period, from years 70–90 annual rainfall is relatively high, allowing wood biomass growth. However, grass biomass is unable to respond to this relatively wet period. The lack of grass recovery following the drought is associated with the combination of grass degradation by low rainfall and competitive effects from wood.

To study how general this result may be, we examine the 100 simulation ensemble from simulation set 1 (uncorrelated rainfall) with conditions of $<P> =$ 650 mm, CV($P$) = 0.6, and an intermediate grazing intensity ($L_g = 0.3$ yr$^{-1}$). This ensemble is chosen for its relatively high, but strongly variable, annual rainfall providing conditions potentially favorable for either grass recovery or sustained degradation. We quantify the degree to which grass recovers from degradation events as follows. First, we calculate the 10-year average of grass biomass, $\tilde{G}_z$, and annual rainfall, $\tilde{P}_s$, following the $z$th degradation event, denoted by subscript $z$ and as identified in the section Interaction of grazing and rainfall effects. Then, to evaluate how grass recovery is influenced by both annual rainfall as well as the wood biomass state at the time of degradation, $W_z$, we calculate the average of $\tilde{G}_z$ for $l$ classes of $\tilde{P}_z$ and $m$ classes of $W_z$, as

$$\hat{\tilde{G}}_{lm} = \frac{\sum_1^{N_z} Y_z \tilde{G}_z}{\sum Y_z}, \tag{6}$$

where

$$Y_z = \left\{ \begin{array}{ll} 1 & \text{for } P^*_l < \tilde{P}_z \le P^*_{l+1} \text{ and } W^*_m < W_z \le W^*_{m+1} \\ 0 & \text{otherwise} \end{array} \right\}, \tag{7}$$

and $P^* = \{0, 100, 200, 300, 400, 500, 600, 700, 800, 900, 1000\}$, $W^* = \{0, 0.5, 1.0, 1.5, 2.0, 2.5, 3\}$ with units of mm

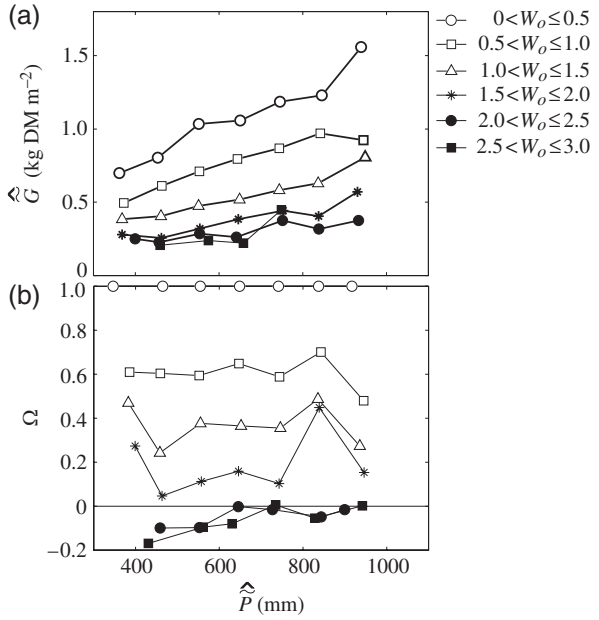


**Fig. 10** (a) Ten-year average grass biomass ($G$), denoted $\tilde{G}$, vs. 10-year average annual rainfall, and (b) the fraction of potential $G$ recovery within 10 years following a degraded state, $\omega$, vs. 10-year average annual rainfall. The symbol ^ denotes that data are averaged within rainfall and initial wood biomass ($W_0$) classes. Mean annual rainfall is 650 mm, coefficient of variation of annual rainfall is 0.7, and grazing intensity is 0.3 yr$^{-1}$.

and kg DM m$^{-2}$, respectively, and $N_z$ is the number of $z$ degradation events. Finally, we quantify the degree to which grass recovers relative to its potential recovery in the absence of wood, hereafter called fractional recovery, as

$$\Omega_{lm} = \frac{\hat{\tilde{G}}_{lm} - G_{cr}}{\hat{\tilde{G}}_{l1} - G_{cr}}, \quad (8)$$

where we note that $\tilde{G}_{l1}$, with (subscript $m = 1$), refers to the 10-year average grass biomass following degradation for the case of wood biomass near zero at the time of degradation.

The initial wood biomass state has a pronounced negative effect on grass recovery (Fig. 10a, b) with high wood biomass strongly suppressing grass recovery following degradation. Grass recovers more completely and to a higher average state in the 10 years following a degraded condition for high rainfall and for low wood biomass (Fig. 10a, b). Furthermore, continued low rainfall over the decade following a degradation event maintains a relatively low grass biomass, even if the wood state is low. These results support a general pathway of woody encroachment (Livingstone, 1991; Brown & Archer, 1999; Fynn & O'Connor, 2000; Roques *et al.*, 2001; Hibbard *et al.*, 2003), whereby wood expands when grass biomass is low and has relatively little competitive effect such as following drought periods or in presence of intense grazing. Such woody expansion may result in hysteresis of grass recovery or potentially persistent wood dominance since grass in a degraded condition may be unable to displace wood, if it can displace wood vegetation at all. Wood is believed to expand in the absence of grass competition for soil water as well as with reduced grass-supported fires that would otherwise kill wood seedlings and saplings (Scholes & Archer, 1997; Higgins *et al.*, 2000). This indicates that periods of low grass cover following persistent dry periods likely lead to events of wood encroachment. In fact, observations show pulses of shrub recruitment (Prins & van der Jeugd, 1993; Roques *et al.*, 2001) that can be linked to periods of high rainfall (Archer *et al.*, 1988; O'Connor, 1995). The findings we present here are consistent with this general pathway of woody encroachment.

## Conclusions

Overall, our results exhibit sensitivity of the dryland system to variability in annual rainfall, particularly when this variability is concentrated in long period rainfall cycles. Variability in annual rainfall reduces the average grass biomass, increases its variability, increases vulnerability to degradation by grazing, and generally increases the likelihood and duration of transition to a low grass condition, enabling wood expansion. Grass recovery from such a degraded condition lags behind improved rainfall conditions especially in the presence of high wood biomass.

These results demonstrate how a minimalistic approach is useful for identifying system sensitivity to forcing. In this case, the model system can be used to identify dryland ecosystems that are particularly sensitive to projected increases in rainfall variability, such as an intensification of decadal-scale climate oscillations. Another opportunity that was outside the scope of the current study is an examination of climate variation concentrated not just in a single timescale, but populating multiple timescales, such as 6- and 20-year oscillations that may generate constructive or destructive cross-scale interactions in system response. Furthermore, the approach enables quantification of system response such as lag time to recovery or fractional resonance with variability in forcing. These measures may be used to characterize and classify ecosystem responses to climate and land use conditions, thus bringing into light areas of concern that merit focused attention. Detailed follow-up examination of these areas of concern could ensue with an improved model system

that better represents the local dynamics, such as competitive interactions, growth and decay, and recolonization or mortality, as typical of an individual-based framework. As such, this study provides a step in the broader direction of diagnosing dryland ecosystem sensitivity to and likely effects of evolving climate and land use pressures.

## Acknowledgements

This research was supported in part by the Biological and Environmental Research (BER) Program, US Department of Energy, through the Southeast Regional Center (SERC) of the National Institute for Global Environmental Change (NIGEC) under Cooperative Agreement no. DE-FC02-03ER63613, and by the National Science Foundation under Grant No. 0243598.

## References

Anderies JM, Janssen MA, Walker BH (2002) Grazing management, resilience, and the dynamics of a fire-driven rangeland system. *Ecosystems*, **5**, 23–44.

Anderson JE, Inouye RS (2001) Landscape-scale changes in plant species abundance and biodiversity of a sagebrush steppe over 45 years. *Ecological Monographs*, **71**, 531–556.

Archer S (1989) Have southern Texas savannas been converted to woodlands in recent history. *American Naturalist*, **134**, 545–561.

Archer S, Scifres C, Bassham CR *et al*. (1988) Autogenic succession in a sub-tropical savanna – conversion of Grassland to Thorn Woodland. *Ecological Monographs*, **58**, 111–127.

Atjay GL, Ketner P, Duvigneaud P (1979) Terrestrial primary production and phytomass. In: *The Global Carbon Cycle, SCOPE*, Vol. 13 (eds Bolin B, Degends ET, Kempe S, Ketner P), pp. 129–181. John Wiley & Sons, Chichester.

Brown JR, Archer S (1999) Shrub invasion of grassland: recruitment is continuous and not regulated by herbaceous biomass or density. *Ecology*, **80**, 2385–2396.

Cao MK, Zhang QF, Shugart HH (2001) Dynamic responses of African ecosystem carbon cycling to climate change. *Climate Research*, **17**, 183–193.

Caylor KK, Shugart HH, Dowty PR *et al*. (2003) Tree spacing along the Kalahari transect in southern Africa. *Journal of Arid Environments*, **54**, 281–296.

Chesson P, Gebauer RLE, Schwinning S *et al*. (2004) Resource pulses, species interactions, and diversity maintenance in arid and semi-arid environments. *Oecologia*, **141**, 236–253.

Easterling DR, Meehl GA, Parmesan C *et al*. (2000) Climate extremes: observations, modeling, and impacts. *Science*, **289**, 2068–2074.

Eaton D (unpublished) Daily rainfall data from 1973 to 2002 near Ghanzi, Botswana.

Edelstein-Keshet L (1988) *Mathematical Models in Biology*. Random House, New York.

Ellis J, Galvin KA (1994) Climate patterns and land-use practices in the dry zones of Africa. *BioScience*, **44**, 340–349.

Ellis JE, Swift DM (1988) Stability of African pastoral ecosystems: alternate paradigms and implications for development. *Journal of Range Management*, **41**, 450–459.

Fisher MJ, Rao IM, Ayarza MA *et al*. (1994) Carbon storage by introduced deep-rooted grasses in the South-American savannas. *Nature*, **371**, 236–238.

Friedel MH (1991) Range condition assessment and the concept of thresholds: a viewpoint. *Journal of Range Management*, **44**, 422–426.

Fuhlendorf SD, Briske DD, Smeins FE (2001) Herbaceous vegetation change in variable rangeland environments: the relative contribution of grazing and climatic variability. *Applied Vegetation Science*, **4**, 177–188.

Fynn RWS, O'Connor TG (2000) Effect of stocking rate and rainfall on rangeland dynamics and cattle performance in a semi-arid savanna, South Africa. *Journal of Applied Ecology*, **37**, 491–507.

Gonzalez P (2001) Desertification and a shift of forest species in the West African Sahel. *Climate Research*, **17**, 217–228.

Grist J, Nicholson SE, Mpolokang A (1997) On the use of NDVI for estimating rainfall fields in the Kalahari of Botswana. *Journal of Arid Environments*, **35**, 195–214.

Grover HD, Musick HB (1990) Shrubland encroachment in Southern New-Mexico, USA – an analysis of desertification processes in the American southwest. *Climatic Change*, **17**, 305–330.

Hibbard KA, Schimel DS, Archer S *et al*. (2003) Grassland to woodland transitions: integrating changes in landscape structure and biogeochemistry. *Ecological Applications*, **13**, 911–926.

Higgins SI, Bond WJ, Trollope WSW (2000) Fire, resprouting and variability: a recipe for grass–tree coexistence in savanna. *Journal of Ecology*, **88**, 213–229.

IPCC (2001) Climate Change 2001: Synthesis Report, Third Assessment Report of the Intergovernmental Panel on Climate Change.

Jackson RB, Banner JL, Jobbagy EG *et al*. (2002) Ecosystem carbon loss with woody plant invasion of grasslands. *Nature*, **418**, 623–626.

Jeltsch F, Weber GE, Grimm V (2000) Ecological buffering mechansims in savannas: a unifying theory of long-term tree-grass coexistence. *Plant Ecology*, **161**, 161–171.

Karl TR, Knight RW, Plummer N (1995) Trends in high-frequency climate variability in the 20th-century. *Nature*, **377**, 217–220.

Knapp AK, Fay PA, Blair JM *et al*. (2002) Rainfall variability, carbon cycling, and plant species diversity in a mesic Grassland. *Science*, **298**, 2202–2205.

Lauenroth WK, Sala OE (1992) Long-term forage production of North-American shortgrass steppe. *Ecological Applications*, **2**, 397–403.

Laycock WA (1991) Stable states and thresholds of range condition on North Amercian rangelands: a viewpoint. *Journal of Range Management*, **44**, 427–433.

Le Houérou HN, Bingham RL, Skerbek W (1988) Relationship between the variability of primary production and the variability of annual precipitation in world arid lands. *Journal of Arid Environments*, **15**, 1–18.

Livingstone I (1991) Livestock management and 'overgrazing' among pastoralists. *Ambio*, **20**, 80–85.

Manzano MG, Navar J, Pando-Moreno M *et al*. (2000) Overgrazing and desertification in northern Mexico: highlights on northeastern region. *Annals of Arid Zone*, **39**, 285–304.

Milchunas DG, Forwood JR, Lauenroth WK (1994) Productivity of long-term grazing treatments in response to seasonal precipitation. *Journal of Range Management*, **47**, 133–139.

Noy-Meir I (1973) Desert ecosystems: environment and producers. *Annual Review of Ecological Systems*, **4**, 25–44.

Noy-Meir I (1975) Stability of grazing systems: an application of predator prey graphs. *Journal of Ecology*, **63**, 459–481.

O'Connor TG (1991) Local extinction in perennial grasslands: a life-history approach. *American Naturalist*, **137**, 753–773.

O'Connor TG (1995) Acacia karoo invasion of grassland – environmental and biotic effects influencing seedling emergence and establishment. *Oecologia*, **103**, 214–223.

Paruelo JM, Lauenroth WK, Burke IC *et al*. (1999) Grassland precipitation-use efficiency varies across a resource gradient. *Ecosystems*, **2**, 64–68.

Pickup G (1996) Estimating the effects of land degradation and rainfall variation on productivity in rangelands: an approach using remote sensing and models of grazing and herbage dynamics. *Journal of Applied Ecology*, **33**, 819–832.

Polakow DA, Dunne TT (1999) Modelling fire-return interval T: stochasticity and censoring in the two-parameter Weibull model. *Ecological Modelling*, **121**, 79–102.

Prins HHT, van der Jeugd HP (1993) Herbivore population crashes and woodland structure in East Africa. *Journal of Ecology*, **81**, 305–314.

Roques KG, O'Connor TG, Watkinson AR (2001) Dynamics of shrub encroachment in an African savanna: relative influences of fire, herbivory, rainfall and density dependence. *Journal of Applied Ecology*, **38**, 268–280.

Roughgarden J (1979) *Theory of Population Genetics and Evolutionary Ecology: An Introduction*. MacMillan Publishing Co., Inc., New York.

Ryerson DE, Parmenter RR (2001) Vegetation change following removal of keystone herbivores from desert grasslands in New Mexico. *Journal of Vegetation Science*, **12**, 167–180.

Scheffer M, Carpenter S, Foley JA *et al*. (2001) Catastrophic shifts in ecosystems. *Nature*, **413**, 591–596.

Scheffer M, Carpenter SR (2003) Catastrophic regime shifts in ecosystems: linking theory to observation. *Trends in Ecology & Evolution*, **18**, 648–656.

Schlesinger WH (1990) Biological feedbacks in global desertification. *Science*, **247**, 1043–1048.

Scholes RJ (1990) Change in nature and the nature of change: interactions between terrestrial ecosystems and the atmosphere. *South African Journal of Science*, **86**, 350–354.

Scholes RJ, Archer SR (1997) Tree-grass interactions in savannas. *Annual Review of Ecology and Systematics*, **28**, 517–544.

Scholes RJ, Kendall J, Justice CO (1996) The quantity of biomass burned in Southern Africa. *Journal of Geophysical Research – Atmospheres*, **101**, 23667–23676.

Trollope WSW, Trollope LA, Potgieter AFL *et al*. (1996) SAFARI-92 characterization of biomass and fire behavior in the small experimental burns in the Kruger National Park. *Journal of Geophysical Research – Atmospheres*, **101**, 23531–23539.

van de Koppel J, Rietkerk M (2004) Spatial interactions and resilience in arid ecosystems. *American Naturalist*, **163**, 113–121.

van de Koppel J, Rietkerk M, Weissing FJ (1997) Catastrophic vegetation shifts and soil degradation in terrestrial grazing systems. *Trends in Ecology & Evolution*, **12**, 352–356.

van Langevelde F, van de Vijver C, Kumar L *et al*. (2003) Effects of fire and herbivory on the stability of savanna ecosystems. *Ecology*, **84**, 337–350.

Walker BH, Ludwig D, Holling CS *et al*. (1981) Stability of semi-arid savanna grazing systems. *Journal of Ecology*, **69**, 473–498.

Wiens JA (1984) On understanding a non-equilibrium world: myth and reality in community patters and processes. In: *Ecological Communities: Conceptual Issues and the Evidence* (eds Strong DR, Simberlong D Jr, Abele KG, Thistle AB), pp. 439–458 Princeton University Press, Princeton, NJ.

West NE (1993) Biodiversity of rangelands. *Journal of Range Management*, **46**, 2–13.

Westoby M, Walker B, Noy-Meir I (1989) Range management on the basis of a model which does not seek to establish equilibrium. *Journal of Arid Environments*, **17**, 235–239.

Wiegand T, Milton SJ (1996) Vegetation change in semiarid communities – simulating probabilities and time scales. *Vegetatio*, **125**, 169–183.

Williams CA, Albertson JD (2004) Soil moisture controls on canopy-scale water and carbon fluxes in an African savanna. *Water Resources Research*, **40**, 1–14.

Williams CA, Albertson JD (2005) Contrasting short- and long-time scale effects of vegetation dynamics on water and carbon fluxes in water-limited ecosystems. *Water Resources Research*. Water Resources Research, **41**, W06005, doi: 10.1029/2004WR003750.

Wu JG, Marceau D (2002) Modeling complex ecological systems: an introduction. *Ecological Modelling*, **153**, 1–6.

Zeng N, Hales K, Neelin JD (2002) Nonlinear dynamics in a coupled vegetation-atmosphere system and implications for desert-forest gradient. *Journal of Climate*, **15**, 3474–3487.

## Appendix A. Growth model parameterization

In water-limited ecosystems, rainfall is recognized as the dominant control on grass and wood net primary productions ($NPP_g$, $NPP_w$, kg DM $m^{-2}$), equivalent to annual vegetation growths. Rainfall also influences ecosystem carrying capacity (e.g. Noy-Meir, 1973; Le Houérou *et al*., 1988; Scholes & Archer, 1997). We include this effect as

$$\begin{aligned} r_x &= \min(a_x P + b_x, r_{x\max}), \\ k_x &= c_x P + d_x, \end{aligned} \tag{A1}$$

where the subscript $x$ refers to grass (g) or wood (w), $r_x$ is the growth rate, $k_x$ is the site-level ecosystem carrying capacity. To obtain the form and parameters for Eqn (A1), we first used the daily time-step model described in Williams & Albertson (2005) to simulate $G$ and $W$ annual growth, denoted as $NPP_x$, for a factorial combination of $G$ and $W$ static states and for five levels of fixed $P$, representing the minimum, lower quartile, mean, upper quartile, and maximum $P$ obtained in the 30-year rainfall record from Ghanzi, Botswana (Eaton, unpublished). Using results from simulations with $G$ in the absence of $W$, and the reverse, we adjusted $r_x$ and $k_x$ to fit the annual

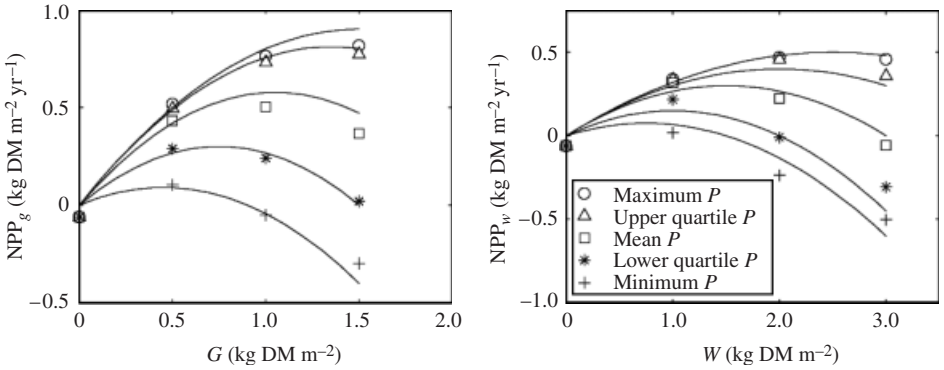


**Fig. A1** Annual net primary production for grass ($NPP_g$) and wood ($NPP_w$), equivalent to annual growth, estimated from the daily time-step model (symbols) as a function of grass biomass ($G$) or wood biomass ($W$) for five levels of annual rainfall ($P$) ranging from the Ghanzi record minimum to maximum (legend), with curves obtained from fitting the annual model to the annual results from the daily time-step model.

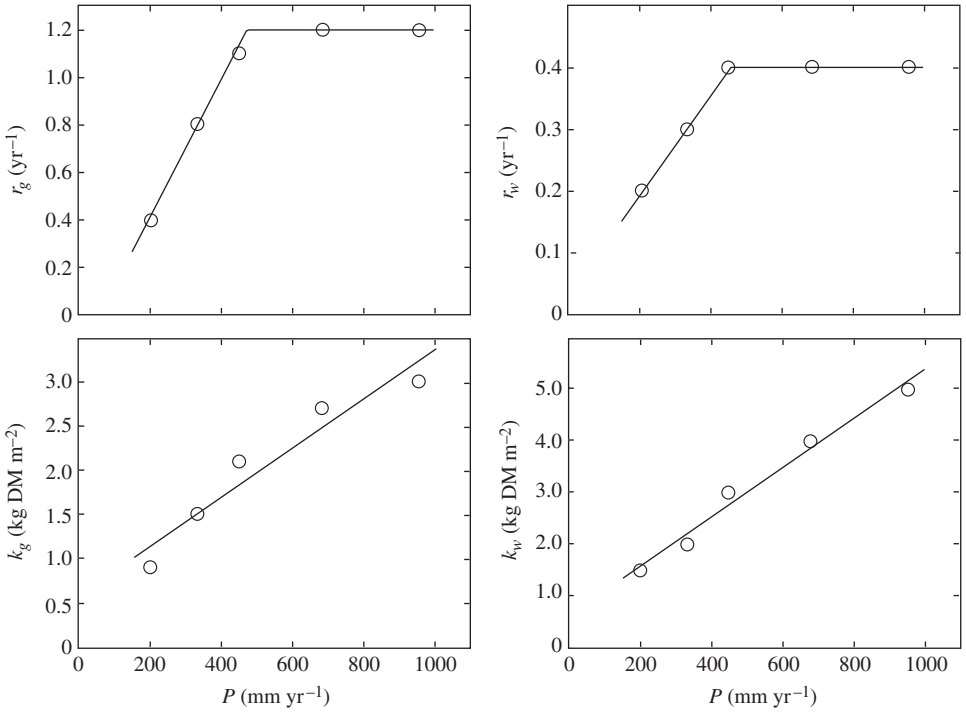


**Fig. A2** Grass and wood growth rates ($r_g$, $r_w$) and carrying capacities ($k_g$, $k_w$) vs. annual rainfall ($P$) obtained from the annual model (line) fit to the annualized daily time-step model (open symbols).

model Eqn (1) to results from the daily time-step model (Fig. A1). The resultant relationships of $r_x$ and $k_x$ with $P$ provided Eqn (A1) and its parameters (Fig. A2). Adopting competition coefficients ($\alpha_w$, $\alpha_g$) similar to Anderies *et al*. (2002), but symmetric as suggested from Williams & Albertson (2005), annual growth from the annual model was in good agreement with that from the daily model for a broad range of $G$, $W$, and $P$, conditions with $R^2$ of 0.83 and 0.87 for $NPP_g$ and $NPP_w$, respectively (Fig. A3).

## Appendix B. Fire model

Scholes *et al*. (1996) estimated mean fire return time ($T_f$, yr), as a function of $<P>$ in southern Africa, related since $<P>$ is a major control of vegetation fuel load. We combined the $<P>$ and $T_f$ relationship of Scholes *et al*. (1996) with a $<P>$ and vegetation cover, $f_v$, relationship in southern Africa described in Caylor *et al*. (2003) to estimate mean fire return time as a

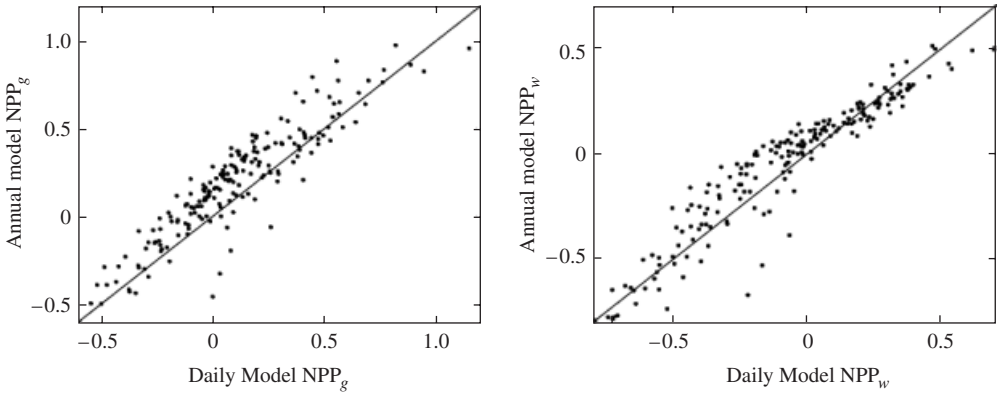


**Fig. A3** Grass and wood annual net primary productions (NPP$_x$, kg DM m$^{-2}$ yr$^{-1}$) from the annual model vs. that from the daily time-step model.

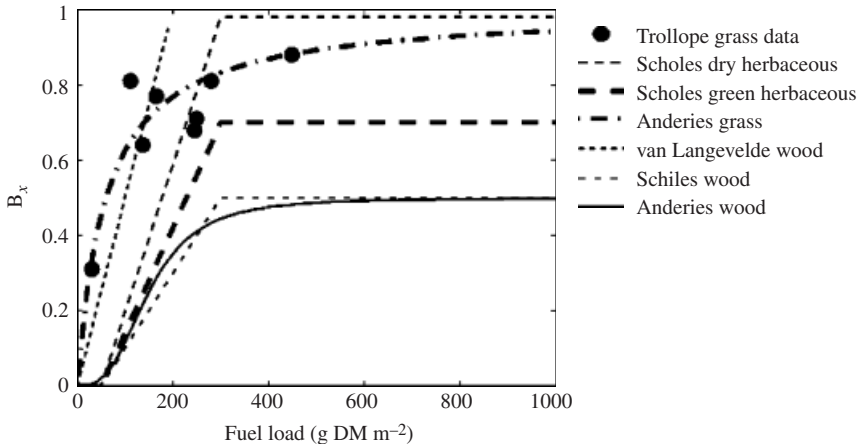


**Fig. B1** Burn completeness ($B_x$, yr$^{-1}$) vs. fuel load for data from a grass fire reported in Trollope *et al*. (1996), and modeled for infertile savannas in Scholes *et al*. (1996), grazing lands based on Anderies *et al*. (2002) but modified as described in this study, and for wood in savannas as in van Langevelde *et al*. (2003).

function of $f_v$, as

$$T_f = 1.75 f_{\mathrm{v}}^{-1.35}, \tag{B1}$$

where

$$f_{\mathrm{v}} = \frac{G}{G_{\max}} + \frac{W}{W_{\max}}, \tag{B2}$$

as in Williams & Albertson (2005). Since fire occurrence is a stochastic process (e.g. Polakow & Dunne, 1999), we modeled annual fire events, $F$, as

$$F = \left\{ \begin{array}{ll} 0 & \text{for} \quad \delta_i > T_f^{-1} \\ 1 & \text{for} \quad \delta_i \leq T_f^{-1} \end{array} \right\}, \tag{B3}$$

where $\delta_i$ is a random variable sampled from a uniform [0, 1] distribution at each time step $i$.

Biomass combustion depends on vegetation combustion completeness factors (Scholes *et al*., 1996) as well as fire intensity, which depends on fuel load (Scholes *et al*., 1996). Figure B1 shows typical relationships combining effects of fire intensity and vegetation-specific combustion completeness factors on the fraction of biomass removed by a fire, hereafter burn completeness. We adopted the two-parameter, continuous function of Anderies *et al*. (2002) that provided a reasonable fit to the Trollope *et al*. (1996) data and was consistent with trends in Scholes *et al*. (1996) (Fig. B1). Unlike the fire model of Anderies *et al*. (2002), we estimated fuel load, and hence fire intensity, with grass and wood covers, not just grass cover, since intense woodland fires can occur even in the absence of grass (Scholes *et al*. 1996). Thus, we modified the Anderies *et al*. (2002) model of burn completeness, $B$, as,

$$B_x = C_x \frac{f_{\mathrm{v}}^{e_x}}{h_x^{e_x} + f_{\mathrm{v}}^{e_x}}, \tag{B4}$$

where $C_x$ is the combustion completeness factor, and $e_x$ and $h_x$ define the sharpness with which $B_x$ increases with $f_v$, and the minimum $f_v$ for burning.